DOI: https://doi.org/10.36722/exc.v1i1.2286

Light-Based Positioning System Using Arduino

Nurul Imam Assidqi[1*], Dwi Astharini[1], Sofian Hamid[1,2]

[1]*Department of Electrical Engineering, Faculty of Science and Technology, University of Al-Azhar Sisingamangaraja, South Jakarta, 12110, Indonesia*
[2]*Institute of High Frequency Technology RWTH Aachen University, Aachen, Germany*
Correspondence Email: imamassidqi@gmail.com

ABSTRACT

The Light Positioning System (LPS) represents an innovative technology employed for precise object localization by utilizing light as a positional reference. This method encompasses the utilization of light sources, such as LED lights or other visible light emitters, which can be strategically positioned at various orientations and angles. This research centers on the practical implementation of the LPS paradigm through the application of Arduino. Additionally, the study involves the integration of the Kalman filter algorithm within the Arduino framework to enhance the accuracy of sensor data estimations. The LPS implementation employs distinct sensors, namely the Photoresistor LM393, Photodiode LM393, and TF-Luna Lidar. The programming is accomplished using the Arduino Integrated Development Environment (IDE), while the hardware framework is based on the Arduino Mega 2560 microcontroller. In this research, the ESP32 module plays a pivotal role as it establishes a seamless connection between the sensor data and the Blynk platform. This integration empowers effective and comprehensive data monitoring and analysis, facilitating real-time tracking and evaluation of the LPS system's performance. The photoresistor exhibits better reading accuracy compared to the photodiode, as evident from the obtained RMSE values. The KF PR with 16 LEDs has the smallest RMSE value, which is 0.03. The TF-Luna LiDAR sensor readings are more accurate and effective under well-lit conditions as opposed to low-light conditions. The RMSE value at lux 160 is 1.41, while the RMSE value at lux 2 is 2.71.

Keywords: ***Light Positioning, Kalman Filter, Arduino Mega 2560, Lidar, Photodetectors, Blynk***

1. INTRODUCTION

In recent years, rapid advancements in communication technology and sensors have driven significant progress in the development of light-based positioning systems, commonly known as Light Positioning Systems (LPS). This technology offers great potential to address challenges in accurately determining positions, particularly in indoor environments or locations with limited GPS signal coverage.

Visible Light Communications (VLC) has emerged as a potential game-changer for the future of wireless communication. VLC utilizes the visible light spectrum (400-700 nm) that serves as an illumination source for transmitting information. The information signal is superimposed on the LED light, ensuring a seamless experience for end-users without any noticeable flickering. This "green" approach combines illumination and communication network connectivity, making VLC an eco-friendly alternative to traditional methods. Moreover, with the growing demand for high-speed wireless access, the exploration of new technologies like VLC has become essential to mitigate the limitations of existing low-frequency bands [1].

VLC-based positioning offers several advantages over traditional radio frequency (RF)-based positioning systems. It can be implemented cost-effectively by utilizing existing lighting systems with minimal modifications. Additionally, VLC positioning is deemed safe for use in areas where RF-based methods might encounter challenges [2].

Visible Light Positioning (VLP) is an accurate indoor positioning technology that

leverages luminaires as transmitters. Circular luminaires are commonly used in VLP but are typically treated as simple point sources for positioning, disregarding their geometry characteristics, which can impact the accuracy of the system [3], in recent years, lighting devices have undergone a revolutionary transformation from fluorescent lamps or tubes to light-emitting diodes (LEDs) because of the energy efficiency for the delivered light output, and the low cost and long lifetime of the LED. Visible light has the double functions of the dominant illumination source and indoor positioning. Visible light positioning (VLP) systems can overcome several known problems with the RF-based indoor positioning system. A receiver cannot receive signals from nearby rooms. Therefore, the positioning algorithm will only use information that is transmitted inside the room in which it needs to calculate its position [4].

VLP accuracy may suffer from insufficient visible light access points (APs) or LEDs. To enhance the accuracy of the VLP, Kalman filters (KFs) can be used. The KF predicts the user location based on previous locations and combines the predictions with the actual measurements to cancel out the negative effects of instantaneous bad measurements. It can track the user efficiently in case the localization method itself fails to do so. However, estimation methods and/or parameters change frequently in many applications. To incorporate these changes into the KF, adaptive estimation can be used [5].

The Kalman filter has been widely studied and employed in various engineering fields since the 1970s. It has garnered significant interest from the industrial electronics community, especially in trajectory estimation, state and parameter estimation for control or diagnosis, data merging, signal processing, and other applications. Researchers have continually worked on improving the performance and stability of the Kalman filter, optimizing computation time, and exploring effective implementations [6].

In light of these advancements, the implementation of a Light Positioning System using Arduino presents an intriguing and promising project. Arduino, as a versatile and popular microcontroller platform, can be utilized to develop the proposed LP system. This project aims to enhance wireless communication in environments with electromagnetic interference (EMI) or for short-range data transfer purposes. The incorporation of the Kalman filter into the Arduino system offers the potential to improve accuracy, sensor efficiency, and overall performance, making it a valuable addition to sensor-based estimation processes.

A photoresistor, also known as an LDR (Light Dependent Resistor), is a semiconductor component whose resistance changes according to the intensity of light falling on it. The LM393 Photosensitive Light-Dependent Control Sensor LDR Module uses a high-quality LM393 voltage comparator. Easy to install using the sensitive type photosensitive resistance sensor the comparator output signal gives a clean and good waveform. Driving ability is 15mA with the adjustable potentiometer, it can adjust the brightness of the light. The working voltage is 3.3V to 5V. Where output is a digital switch output [7].

The photodiode can effectively detect the ambient light's brightness and intensity. In comparison with a photoresistor, it exhibits excellent directivity, enabling it to precisely perceive the fixed direction of the light source. Additionally, its sensitivity can be adjusted through a digital potentiometer. The photodiode operates within a voltage range of 3.3V to 5V and offers digital switch outputs represented by values 0 and 1 [8].

TF-Luna is a single-point ranging LiDAR, based on the TOF (Time of Flight) principle. It is mainly used for stable, accurate, and high-frame-rate range detection. This LiDAR is built with algorithms adapted to suit various application environments and offers excellent distance measurement performances in complex application fields and scenarios. It also supports two interfaces for communication: UART and I2C and the configurations and parameters on this LiDAR can be adjusted according to the application needed. TF-Luna is based on TOF, namely, the Time of Flight principle. It emits modulation waves of near-infrared rays periodically, which will be reflected after contact with an object. The LiDAR obtains the time of flight by measuring the round-trip phase difference and then calculates the relative distance between the LiDAR and the detected object [9], this study also discusses the implementation of the Kalman filter for the integrated Light Positioning System on the Arduino platform, enabling enhanced accuracy and efficiency of sensor (photodetector & Tf-Luna Lidar) measurements, analyzing the performance of the system involving sensor and

data estimation, exploring indoor positioning and wireless communication, and opening up new possibilities for various applications.

Based on the research and development conducted by UAI before regarding the application of KF to the 3D indoor positioning system which can be seen in [10], UAI has also implemented a VLC Transmitter and Receiver Point Using Xilinx FPGA (Field Programmable Gate Array) which can be seen in [11], The problem discussed in this project is to explore how effective the implementation of Kalman Filter into the light positioning system using Arduino.

2. METHOD

Framework Research

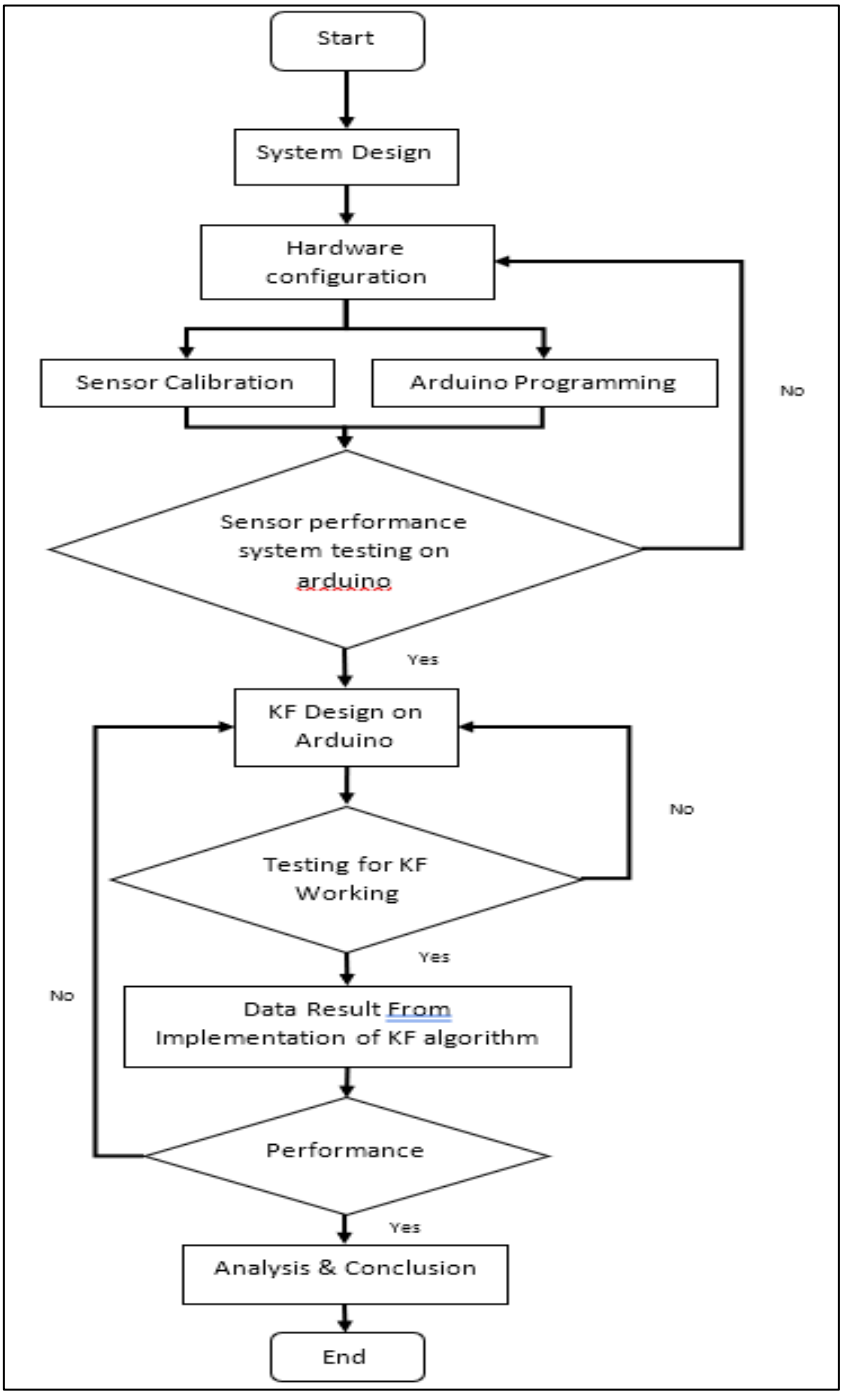

Figure 1. Framework of Research

The research commenced with a comprehensive literature review on Visible Light Positioning, Sensors used (PD & LiDAR), Kalman Filter, Arduino, Esp32, and Blynk to establish a strong theoretical foundation for the study. Subsequently, a system design was meticulously developed for light-based Positioning, which was further implemented and configured using the Arduino Mega platform. Once the Arduino program was meticulously crafted, rigorous testing was conducted using photodetector or lidar sensors as receivers to acquire experimental data.

The collected data was then meticulously processed through the Arduino Integrated Development Environment (IDE) and displayed on the computer through the serial monitor. After successful testing, the subsequent step involved the meticulous implementation of the Kalman Filter into the program to enhance the accuracy and reliability of the acquired data. The gathered data was then subjected to in-depth analysis, and graphical representations were thoughtfully generated to facilitate a comprehensive understanding of the results. From the analyzed data and findings, meaningful conclusions were drawn, which were subsequently thoughtfully integrated into the final project report. This systematic approach ensured the scientific rigor and validity of the study, and the project's outcomes hold promise for advancements in the field of light-based Positioning and its applications in various domains.

System Design

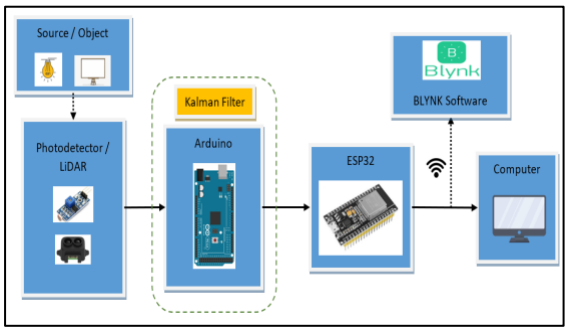

Figure 2. System Design of Complete KF LP Implementation

Shows the system design that will be made in this project. The implementation process of the Light Positioning (LP) system with Kalman Filter begins with the utilization of photodetectors sensors as receivers to read light data emitted by LEDs or LiDAR sensors to detect the object at a distance. The acquired light-intensity data is then processed through an Arduino Mega microcontroller, where the Arduino Mega acts as the main processing unit. The processed data is displayed via the serial monitor for monitoring and verification purposes.

Once the LP system is successfully implemented and proven to function adequately, the next step involves integrating the Kalman Filter program into the Arduino microcontroller. This Kalman Filter is responsible for estimating position data based on the previously obtained light intensity data. By utilizing the Kalman Filter, it is expected that the position of the monitored object or device can be estimated with higher accuracy and closer to the actual value.

After the Kalman Filter implementation process is successfully carried out, the estimated data from the Arduino will be transmitted through communication modules such as ESP32. The ESP32 acts as a data transmitter device, which transmits data through a selected Internet of Things (IoT) platform, such as Blynk. This IoT platform will receive data from the ESP32 and subsequently perform further data processing as required.

The processed data through the IoT platform will then be transformed into graphs to visualize the estimated position data. These graphs will be displayed on a computer or other connected devices through the IoT platform, enabling real-time data monitoring and analysis. With this systematic approach, it is anticipated that the VLP system with Kalman Filter Implementation can provide more accurate and reliable position estimation results, enabling the use of this data in various applications that require high-precision position detection and estimation.

Schematic Design

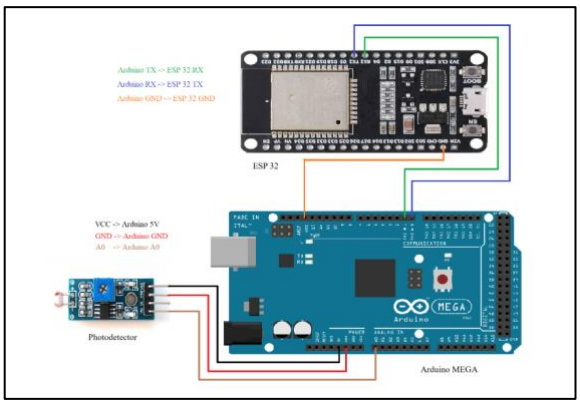

Figure 3. Schematic Design for Photodetector

In the Arduino's utilization in reading data from a photodetector sensor and transmitting sensor data to an ESP32. In this configuration, the VCC voltage of the photodetector is linked to the Arduino's 5V pin, serving as the power source. Furthermore, the ground connection of the photodetector is connected to the Arduino's ground pin, ensuring a shared ground reference between the two devices. Subsequently, the A0 output pin of the photodetector is interconnected with the Arduino's analog pin A0, functioning as an input for data acquisition from the photodetector sensor.

Upon establishing these connections, the Arduino effectively acquires data from the photodetector through the analog pin A0. The collected sensor data is then transmitted to the ESP32 through a designated channel. The data transmission involves connecting the transmit (TX) pin on the Arduino to the receive (RX) pin on the ESP32, and vice versa. Additionally, the ground connection of both devices is interconnected to maintain a common reference potential.

This comprehensive setup enables the Arduino to efficiently read sensor data and subsequently transmit it to the ESP32 for further processing or communication with external platforms. By integrating these two devices, researchers and developers can create sophisticated applications that involve real-time data collection, analysis, and wireless communication. This well-engineered framework showcases the collaborative capabilities of the Arduino and ESP32 platforms, paving the way for innovative solutions in various domains such as the Internet of Things (IoT), sensor networks, and data-driven applications.

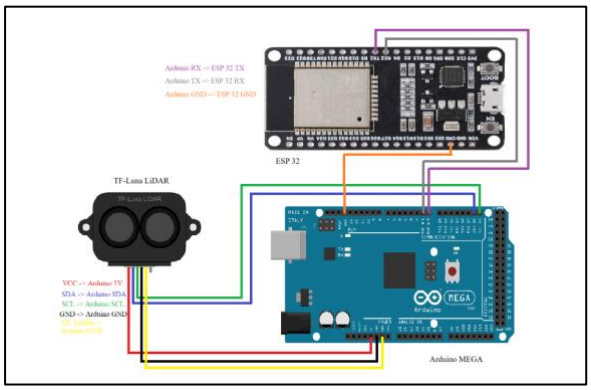

Figure 4. Schematic Design for Tf-Luna LiDAR

The utilization of Arduino in reading data from a photodetector sensor and transmitting the sensor data to an ESP32. In this scheme, the VCC voltage of the photodetector is connected to the Arduino's 5V pin, serving as the power source. Additionally, the ground connection of the photodetector is linked to the Arduino's ground pin, ensuring a common ground reference between the two devices. Subsequently, the A0 output pin of the photodetector is interconnected with the Arduino's analog pin A0, functioning as an input to read data from the photodetector sensor.

Upon establishing these connections, the Arduino efficiently acquires data from the photodetector through the analog pin A0. The collected sensor data is then transmitted to the ESP32 through a designated channel. The data transmission involves connecting the transmit (TX) pin on the Arduino to the receive (RX) pin on the ESP32, and vice versa. Additionally, the ground connection of both devices is interconnected to maintain a common reference potential.

This comprehensive setup enables the Arduino to efficiently read sensor data and subsequently transmit it to the ESP32 for further processing or communication with external platforms. Researchers and developers can create sophisticated applications involving real-time data collection, analysis, and wireless communication by integrating these two devices. This well-engineered framework showcases the collaborative capabilities of the Arduino and ESP32 platforms, paving the way for innovative solutions in various domains such as the Internet of Things (IoT), sensor networks, and data-driven applications.

Kalman Filter Algorithm

Fundamentally, the Kalman Filter algorithm operates by performing two primary stages: the Prediction Stage and the Update Stage. The equations are as follows:

Prediction:

$$\boldsymbol{x_p = A.x_{t-1}} \quad (1)$$

$$\boldsymbol{P_p = A.P_{t-1}.A^T + Q} \quad (2)$$

Update:

$$\boldsymbol{K_t = P_p.C^T.(C.P_p.C^T + R)^{-1}} \quad (3)$$

$$\boldsymbol{x_t = x_p + K_t.(Z_t - C.x_p)} \quad (4)$$

$$\boldsymbol{P_t = (I - K_t.C).P_p} \quad (5)$$

The Prediction Stage is divided into two parts: (a.) Prediction of the Next State involves the equation $\boldsymbol{x_p}=\boldsymbol{A}.\boldsymbol{x_{t-1}}$, which $\boldsymbol{x_p}$ represents the prediction of the next state. Matrix $\boldsymbol{A}$ is the transition matrix that connects the current state $\boldsymbol{x_{t-1}}$ with the prediction of the subsequent state$\boldsymbol{x_p}$. The second part. (b.) Prediction of the Next Covariance pertains to $\boldsymbol{P_p}$, which is the next covariance prediction. $\boldsymbol{P_{t-1}}$ denotes the covariance prediction from the previous iteration. stands for the transpose of the transition matrix $\boldsymbol{A^T}$, and $\boldsymbol{Q}$ is the covariance matrix representing the noise in the prediction model.

The Update Stage is further divided into three parts. (a.) Kalman Gain, where $\boldsymbol{K_t}$ represents the Kalman gain. Matrix $\boldsymbol{C}$ serves as the observation matrix that connects the state $\boldsymbol{(x_p)}$ with the measurement data, and $\boldsymbol{R}$ is the covariance matrix accounting for the actual measurement noise. (b.) Final State Prediction, which $\boldsymbol{x_t}$ signifies the ultimate state prediction, and $\boldsymbol{Z_t}$ is the actual measurement data. (c.) Final Covariance Prediction, where $\boldsymbol{P_t}$ stands for the final covariance prediction, and $\boldsymbol{I}$ denotes the identity matrix. In this project, while in measurements using photodetectors sensors (photoresistor & photodiode), the state x is position (estimated voltage in volts), the state update is in the form of filtered voltage in volts, while in measurements using the tf luna lidar sensor the state is proximity (estimated distance in centimeters), the state update is in the form of filtered distance in centimeters.

3. RESULT AND DISCUSSIONS

This chapter is dedicated to the comprehensive testing conducted, which begins with the design of LEDs as the light source for measurements utilizing photodetector sensors. The ensuing results are presented and subjected to thorough analysis. Furthermore, the integration of the Kalman filter into the Arduino is executed within this testing phase and subsequently scrutinized. Following the assessment of the photodetector sensors, the evaluation proceeds to encompass the utilization of the TF Luna LIDAR sensor on an object, with the subsequent implementation of the Kalman filter. Subsequent stages encompass the computation of Root Mean Square Error (RMSE) for each sensor to gauge the effectiveness of the applied Kalman filter. Lastly, the monitoring of sensor reading outcomes using the Blynk platform is undertaken.

Measurement of Photodetector

The testing process involves the utilization of a photodetector sensor, while the light source is provided by pre-designed LEDs. The photodetector captures light signals emitted by the LEDs, and the resultant data is converted into voltage and processed by the Arduino. Subsequently, this processed data is displayed on the serial monitor. Two types of photodetectors are employed for this experiment: the LM393 photoresistor and the LM393 photodiode.

In this study, an LED system design is implemented to facilitate data transmission via light signals emitted by LEDs. The primary objective of this design is to attain enhanced efficiency and effectiveness in transmitting data through optical signals. To realize this objective, an assemblage of 16 and 8 5mm LEDs is deployed, structured in a configuration of 4x4 and 4x2 respectively. Through this meticulous arrangement of LED elements, the anticipation is that the transmission of data via light signals can be accomplished with optimal precision and efficiency.

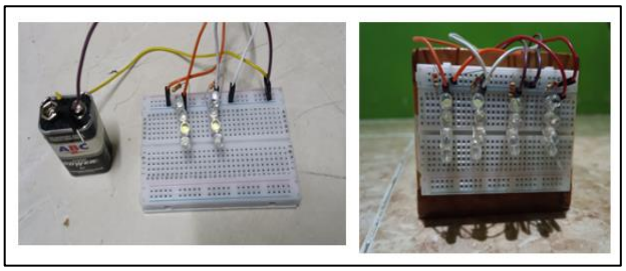

Figure 5. Design LED System

The experimental procedure encompasses data acquisition from the photodetectors, with their positions adjusted at various points within a distance range of 10 cm to 100 cm from the fixed-position LED light source (shown in Figure 4.). Additionally, the light intensity at each point is measured using a lux meter within the same range. To ensure robustness in the results, the experimentation is conducted repetitively, iterated ten times for each configuration. Subsequently, the obtained datasets are averaged to derive representative values, which form the basis for subsequent comprehensive analysis.

Figure 6. Measurement of Photodetector

By following this meticulously structured experimental methodology, this study aims to comprehensively investigate the performance characteristics of the LM393 photoresistor and LM393 photodiode as photodetectors. The systematic variation in positional parameters coupled with precise luminous intensity measurements underpins the validity and reliability of the acquired data. This scientific rigor in data collection sets the stage for a meticulous analysis of the photodetectors' responsiveness and efficacy in varying light conditions.

To comprehensively analyze the performance of the tested system, a thorough comparison of the obtained results is conducted. In this context, two types of sensors, namely Photodiode (PD) and Photoresistor (PR), are the focus of the comparison. Each of these sensors is tested under two different settings measurements against 8 LEDs and 16 LEDs. This comparison aims to identify and deeply analyze the relative performance of each sensor and LED quantity in providing accurate estimations of measurement data.

Table 1. Comparison Measurement Result Of Photoresistor With 16 LED & 8 LED

Photoresistor Distance (cm)	***16 LED Measurement (v)***	***8 LED Measurement (v)***	***16 LED Lux (lx)***	***8 LED Lux (lx)***
10	*0,596*	*0,648*	*1067*	*900,4*
20	*0,9775*	*1,346*	*482*	*304,6*
30	*1,481*	*1,965*	*237,5*	*131,4*
40	*1,945*	*2,511*	*134*	*70,8*
50	*2,314*	*2,914*	*85,5*	*46*
60	2,669	3,215	58	32,4
70	2,969	3,489	42,5	21
80	3,2085	3,69	32	18
90	3,475	3,86	25	16
100	3,637	3,986	20	10,6

Table 2. Comparison Measurement Result of Photodiode with 16 LED & 8 LED

Photodiode Distance (cm)	***16 LED Measurement (v)***	***8 LED Measurement (v)***	***16 LED Lux (lx)***	***8 LED Lux (lx)***
10	*0,098*	*1,7265*	*1072,5*	*859,25*
20	*0,122*	*2,5685*	*458,5*	*240*
30	*0,161*	*3,673*	*225,5*	*132,75*
40	*1,139*	*4,239*	*140,5*	*72,5*
50	*2,605*	*4,495*	*90,5*	*47,75*
60	3,030	4,59	61,5	32,25
70	3,7	4,6388	45	24
80	3,94	4,76	33,5	18,75
90	4,184	4,8105	25,5	15
100	4,462	4,834	21,5	12

Table 1, displays measurement data using PR LM393 with variations of 16 LEDs and 8 LEDs. The data encompasses the distance between PR LM393 and LEDs. Table II depicts measurement data employing PD LM393 with variations of 16 LEDs and 8 LEDs. The data encompasses the distance between PD LM393 and LEDs. Light intensity is measured in lux using a Lux Meter, and output voltage is measured in volts using Arduino Software. The results yield significant insights.

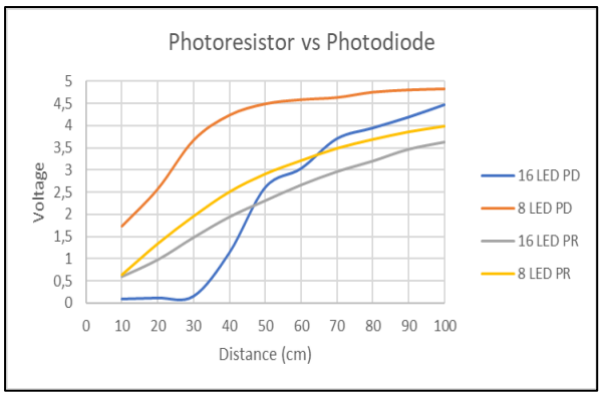

Figure 7. Measurement Result of Photodetectors

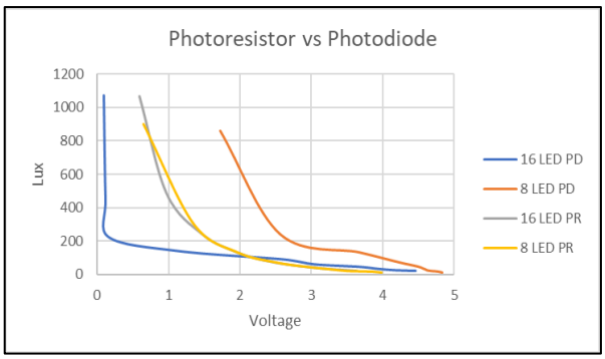

Figure 8. Measurement Result of Photodetectors (lux vs voltage)

This measurement results from two types of sensors: Photoresistor (PR) and Photodiode (PD). Generally, photodiodes exhibit a faster response to changes in light compared to photoresistors because the conductivity of a photodiode changes with the received light, whereas a photoresistor alters its resistance when exposed to light. In the table, it is evident that the voltage produced by the photodiode tends to be higher than that of the photoresistor at the same distance, indicating a greater sensitivity to light.

Typically, as the distance between the sensor and the light source increases, the received light intensity decreases. There is a consistent trend where voltage values generally increase with greater distance between the sensor and the object. This reflects the anticipated relationship between light intensity and distance. Figure 7. also compares measurements between 8 LEDs and 16 LEDs for each sensor. Generally, a higher number of LEDs can result in greater light intensity, which in turn affects the sensor's response. From Figure 4.11, it can be observed that measurements with 16 LEDs yield higher voltages compared to 8 LEDs at the same distance, indicating higher light intensity from a larger number of LEDs.

From Figure 7., it is noticeable that in most measurements, the photodiode with 16 LEDs produces the highest voltage, followed by the photodiode with 8 LEDs, then the photoresistor with 16 LEDs, and finally the photoresistor with 8 LEDs. This suggests that under these measurement conditions, photodiodes exhibit a higher sensitivity to light than photoresistors, and a greater number of LEDs generates higher light intensity.

In general, photodiodes have a faster response to changes in light and a larger dynamic range compared to photoresistors. From Figure 8., it can be observed that the voltage generated by the photodiode is lower than that of the photoresistor at the same distance, even though the Lux value from the photodiode may be higher. This suggests that the photoresistor might be more sensitive to lower light intensities.

The higher Lux values of the photodiode indicate a greater sensitivity to light, despite producing a lower voltage. From Figure 8, it can be seen that at the same distance, using 16 LEDs results in higher Lux values than 8 LEDs for both the photoresistor and photodiode sensors. Increasing the number of LEDs produces higher light intensity, as reflected in the larger Lux values. However, the generated voltage tends to be lower at the same distance.

Kalman Filter Result of Photodetector

This section discusses the implementation of the Kalman Filter algorithm on the Arduino platform. The sensor data utilized originates from a photodetector. Following the deployment of the Kalman Filter program, the Arduino microcontroller processes the aforementioned photodetector data. The processed data is then translated into real-time visualizations, facilitating immediate comprehension by users or pertinent systems.

The data acquisition method employed involved gradually moving the photodetector sensor away from the LED light source in increments, starting from a point of 10 cm and progressively increasing the distance to 20 cm, 30 cm, and so forth, up to 100 cm. Upon reaching the maximum distance, the data collection process continued by moving the sensor back towards the source, starting from 100 cm and

decrementing the distance in sequence until returning to the initial point of 10 cm.

This approach holds significant relevance in data analysis as it allows for a comprehensive understanding of the sensor's response to changes in distance from the light source. By conducting measurements at various distances, trends, and patterns in the sensor's response can be identified, as well as an understanding of how the sensor reacts to changes in light intensity based on its relative position to the light source.

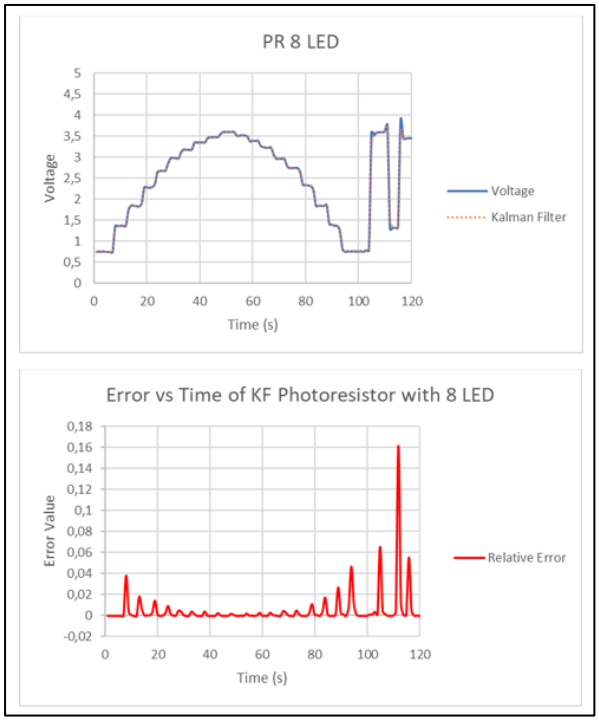

Figure 9. KF Result of Photoresistor with 8 LED

From the provided data in Figure, several observations and analyses can be drawn regarding the comparison between measurement values and the Kalman Filter (KF) method over time. At the beginning of the measurement period, it is evident that the KF values tend to align closely with the actual measurement values. This initial alignment indicates that the KF method does not produce significant changes in the estimated values initially. However, as time progresses, differences between the measurement values and KF estimates begin to emerge. At certain points (such as during the time interval from 103 to 106), significant disparities between the two values become apparent.

Notably, the KF method follows the fluctuations trend present in the measurement data. During specific time intervals (such as from 105 to 109), the KF method effectively mitigates the effects of data fluctuations and generates more stable estimations. In certain instances, KF estimates tend to be lower than the actual measurement values. Nevertheless, within some time intervals (such as from 112 to 114), the KF values and measurements converge and become closer to each other.

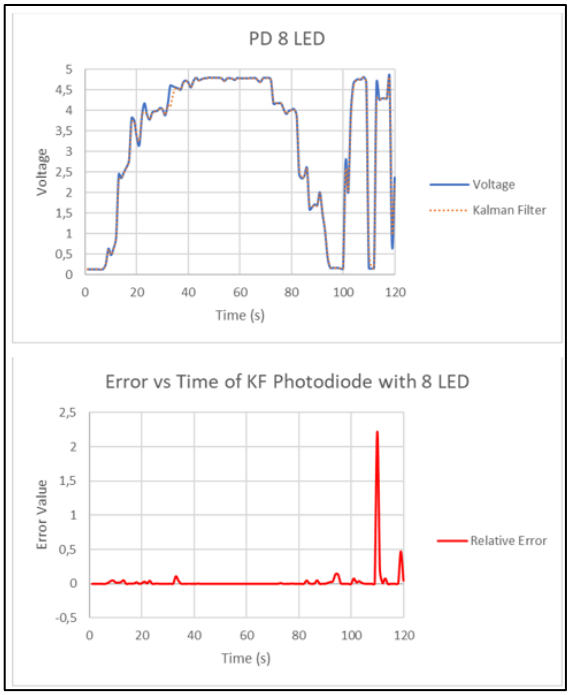

Figure 10. KF Result of Photodiode with 8 LED

From the Figure, a comparison between measurement values and the Kalman Filter (KF) method over time reveals several observations and analyses. At the beginning of the measurement period (time 1-5), the KF values tend to closely track the measurement values. This indicates that initially, the KF method exhibits a response similar to the actual measurement values. In certain time intervals (such as 15-17), the KF method tends to approach the actual measurement values, yet with noticeable disparities. During the time interval of 18-21, significant fluctuations occur in the measurement data, and the KF method does not fully follow these fluctuations. This suggests that the KF method might experience delays in addressing rapid changes in the data.

Despite discrepancies between measurement values and KF estimates for most of the time, at certain points (such as 29-31), it is evident that the KF method successfully tracks the actual measurement values. Within the time interval of 33-36, the KF method exhibits notable differences from the actual measurement values,

indicating greater mismatches in the estimation. Notably, significant fluctuations in the measurement data during the interval of 40-42 also affect KF estimates, yet in some cases (such as 43-44), the KF method manages to approach the measurement values. Towards the end of the measurement period (time interval 100-120), it is apparent that the KF method still retains significant differences from the actual measurement values.

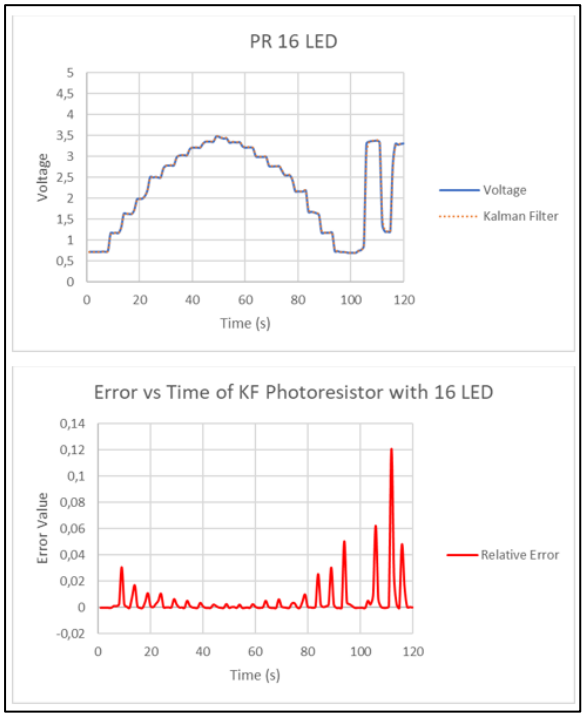

Figure 11. KF Result of Photoresistor with 16 LED

A comparison between measurement values and the Kalman Filter (KF) method over time reveals several observations and analyses. At the beginning of the measurement period (time 1-5), it is evident that the KF method exhibits a response almost identical to the actual measurement values. The difference between KF and the actual measurement values is very minimal. However, during the time interval of 6-12, some fluctuations in the difference between KF and the actual measurement values occur. Despite these fluctuations, the KF method still tends to follow the general trend of the measurement values. It is noticeable that within the time interval of 22-28, the KF method continues to adeptly capture changes in the trend of the measurement data. However, the difference between KF and the actual measurement values slightly increases.

During the time interval of 54-66, fluctuations in the difference between KF and the actual measurement values are observed. The KF method tends to track the general trend, yet these differences persist. Towards the end of the measurement period (time interval 99-120), it is evident that the KF method still manages to follow the general trend of the measurement data, despite fluctuations in the disparities between KF and the actual measurement values.

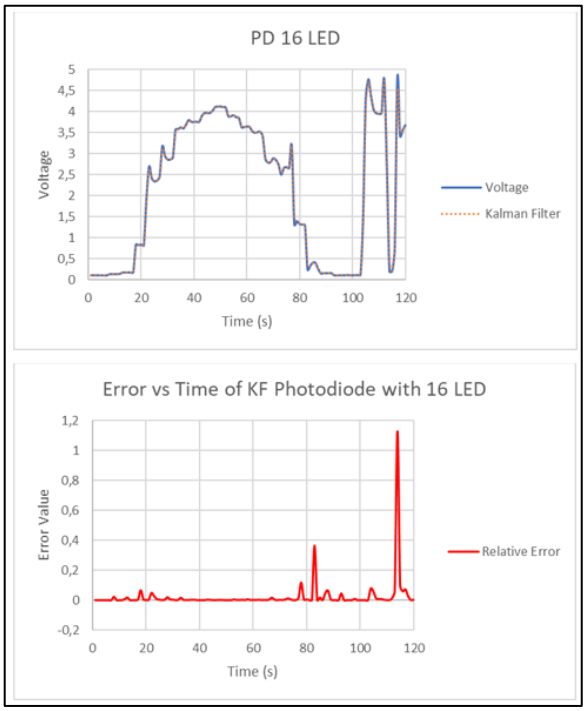

Figure 12. KF Result of Photodiode with 16 LED

There is a dataset comparing measurement values and the Kalman Filter (KF) method over time, and the following observations and analyses can be made: At the beginning of the measurement period (time 1-7), the KF method exhibits a response almost identical to the actual measurement values. The difference between KF and the actual measurement values is minimal. In the time interval of 17-27, the difference between KF and the actual measurement values tends to increase. There are larger fluctuations in these differences, and the KF method might encounter challenges in addressing rapid data fluctuations.

At certain points (such as in the time interval of 42-47), KF successfully approximates or even matches the actual measurement values, but at other points, significant differences remain evident. In the time interval of 67-76, KF exhibits larger disparities from the actual measurement values. Fluctuations in these differences are present, and the KF method might experience delays in adjusting to data

changes. Towards the end of the measurement period (time interval of 83-120), it is evident that the KF method still manages to follow the general trend of the measurement data, despite fluctuations in the disparities between KF and the actual measurement values.

Measurement of TF-Luna LiDAR

This section delves into the discussion regarding the sensor measurement of the TF Luna LiDAR. Real-time data from the TF Luna LiDAR is acquired by the Arduino, providing distance measurements in centimeters. These measurements are conducted within a room measuring 7.6 x 6.4 square meters. The measurements are taken under two distinct conditions: illuminated conditions (light on) when lux is 160 and dark conditions (light off) when lux is 2. Furthermore, the integration of the Kalman filter into the Arduino is also implemented to refine the sensor readings. The focal point of these measurements centers on a whiteboard (object), strategically positioned within the experimental area. The data acquisition process is meticulously orchestrated, involving periodic sensor movement, commencing from the farthest distance and progressively approaching the whiteboard (shown in Figure 13.).

Figure 13. Measurement of TF Luna LiDAR

This analysis aims to systematically portray the experiment conducted using the TF Luna LIDAR sensor under varying environmental conditions. By real-time distance measurements within the specified room dimensions, this study provides a deeper insight into how the sensor's performance alters based on changes in illumination. The utilization of the Kalman filter method within the Arduino represents a commonly employed solution to mitigate noise and enhance the accuracy of sensor readings. The integration of this method signifies a more advanced approach in processing the acquired sensor data, to yield more accurate and consistent measurement results.

The data collection was carried out by gradually moving the TF-Luna LiDAR sensor towards the object. This process began from an initial distance of approximately 7 meters and sequentially approached the object, reducing the distance to 6 meters, 5 meters, and so on until reaching a distance of 1 meter. Subsequently, this procedure was repeated by slowly moving the sensor away from the object, starting from 1 meter and sequentially increasing the distance to 2 meters, and so forth, until returning to the initial point of 7 meters.

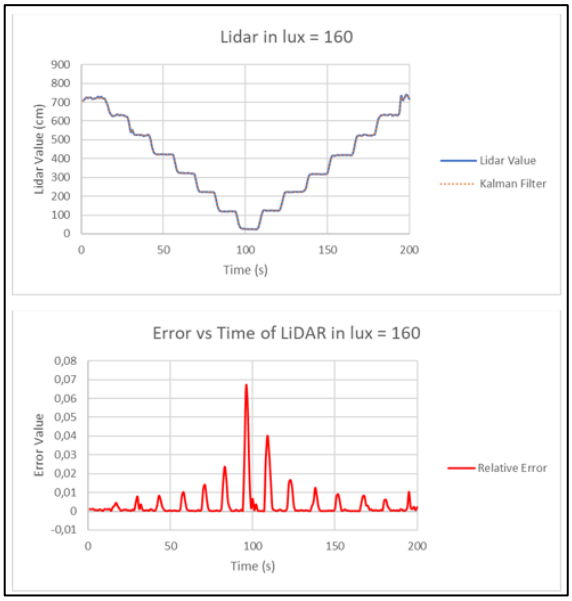

Figure 14, KF Result of TF-Luna LiDAR with conditions light on

There is a dataset comparing Lidar values and the Kalman Filter (KF) method over time, and the following observations and analyses can be made: At the beginning of the measurement period (time 1-7), the difference between Lidar values and KF is very small. KF performs well in closely approximating the initial Lidar values. In the time interval of 17-27, KF manages to follow the general trend of the Lidar data, even though there are larger fluctuations in differences at certain points. In the time interval of 28-48, KF exhibits relatively minor disparities from the Lidar values. KF can approximate the Lidar values effectively despite significant data fluctuations.

In the time interval of 49-66, there are relatively larger fluctuations in the differences between KF and Lidar values. In the time interval of 77-82, the disparities between KF and

Lidar values tend to be larger, but KF still manages to follow the general data trend. In the time interval of 95-101, significant fluctuations in differences between KF and Lidar values are present. In the time interval of 164-187, KF exhibits relatively small differences from Lidar values. In the time interval of 188-200, KF successfully approximates or even matches Lidar values effectively for the majority of points.

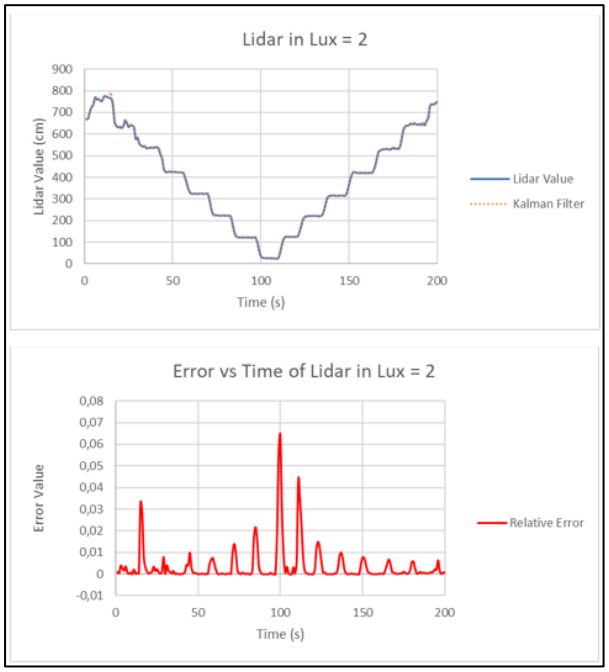

Figure 15. KF Result of TF-Luna LiDAR with conditions light off

The comparison data between Lidar values and the Kalman Filter (KF) method presented in the second measurement, the following observations and analyses can be made: At the beginning of the measurement period (time 1-12), the difference between Lidar values and KF is relatively small, and KF effectively approximates or even matches the Lidar values well. In the time interval of 13-26, there are significant fluctuations in the differences between KF and Lidar values. KF appears to struggle to keep up with rapid fluctuations in the data. In the time interval of 37-44, KF exhibits relatively minor differences from the Lidar values, even though there are fluctuations in differences at certain points.

In the time interval of 61-76, KF successfully approximates the Lidar values effectively, despite fluctuations in differences at certain points. In the time interval of 77-92, the disparities between KF and Lidar values tend to be larger, particularly at points where fluctuations in differences are quite significant. In the time interval of 93-107, KF once again approximates or even matches the Lidar values well for the majority of points. In the time interval of 174-184, the differences between KF and Lidar values tend to be larger, especially at points where fluctuations in differences are quite significant. In the time interval of 185-200, KF once again approximates or even matches the Lidar values well for the majority of points.

Root Mean Square Error (RMSE)

In this context, the computation of RMSE for each outcome resulting from the implementation of the Kalman Filter in the conducted testing will be discussed. This calculation is performed to determine the estimation error of the Kalman Filter in scenarios involving the PR with 8 LEDs, PD with 8 LEDs, PR with 16 LEDs, PD with 16 LEDs, TF-Luna LiDAR with Lux 160, and TF-Luna LiDAR with Lux 2. By juxtaposing the RMSE calculations, the effectiveness of the implemented Kalman Filter can be quantitatively assessed.

The RMSE values provide insights into the disparity between estimated and actual values, serving as a metric to gauge the performance enhancement achieved through the Kalman Filter application. This comparative analysis offers a systematic means to ascertain the filter's efficacy across varied scenarios, shedding light on its capacity to mitigate estimation errors.

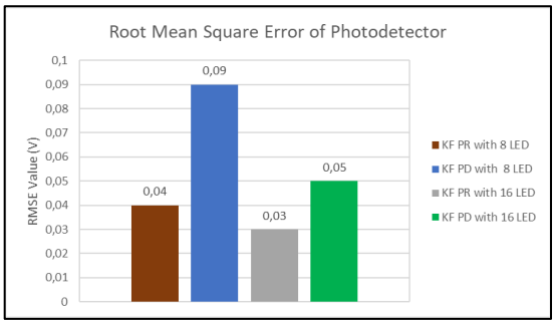

Figure 16. RMSE for Photodetector

Displays the Root Mean Square Error (RMSE) values obtained. It can be observed that in KF PR with 8 LEDs, the RMSE value of 0.04 v indicates that the PR-type Kalman Filter method with 8 LEDs exhibits a high level of accuracy in predicting data. The low RMSE value (0.04 v) signifies that the overall KF estimation closely approximates the true values. For KF PD with 8 LEDs, the RMSE value is

0.09v. The PD-type Kalman Filter method with 8 LEDs has a slightly higher RMSE compared to KF PR with 8 LEDs. Nevertheless, this RMSE value remains relatively low, indicating that this method also provides reasonably accurate estimations.

Meanwhile, in KF PR with 16 LEDs, the RMSE value is 0.03 v. The PR-type Kalman Filter method with 16 LEDs yields a lower RMSE compared to KF PR with 8 LEDs. This suggests that an increase in the number of LEDs can contribute to enhancing KF estimation accuracy. Moving on to KF PD with 16 LEDs, the RMSE value is 0.05 v. The PD-type Kalman Filter method with 16 LEDs has a slightly higher RMSE compared to KF PR with 16 LEDs. However, similar to the case of KF PD with 8 LEDs, this RMSE value remains within an acceptable range.

In the comparison between KF PR and KF PD, it is evident that KF PR tends to provide more accurate estimations in terms of RMSE, particularly for both LED configurations (8 and 16). The number of LEDs also impacts accuracy, as an increase in LED count tends to reduce the RMSE value, indicating an enhancement in estimation accuracy.

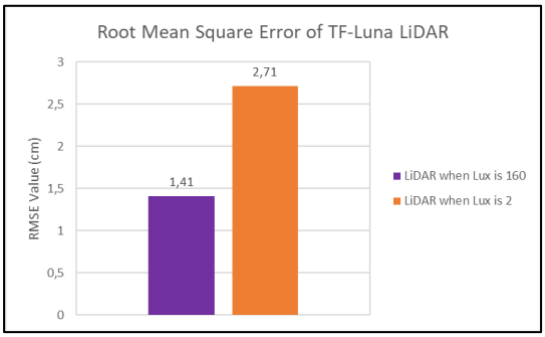

Figure 17. RMSE for TF-Luna LiDAR

Which presents the obtained Root Mean Square Error (RMSE) values, it can be observed that for TF-Luna LiDAR when lux is 160, the RMSE value is 1,41 cm. This RMSE value indicates the extent to which the estimation from the TF-Luna LiDAR sensor approximates the true value when the light intensity reaches 160 lux. The relatively low RMSE value (1,41 cm) signifies that the sensor provides fairly accurate estimations under this light intensity condition. For TF-Luna LiDAR when lux is 2, the RMSE value is 2,71. This RMSE value is higher compared to the previous condition. It indicates that the performance of the TF-Luna LiDAR sensor becomes less accurate when the light intensity is very low (2 lux). Although the RMSE value still falls within a certain range, the increase in RMSE suggests that the sensor might face challenges in accurately measuring distances under very low light intensities. This analysis demonstrates that the performance of the TF-Luna LiDAR sensor is influenced by light intensity. The sensor may be more accurate in measuring distances under higher light intensity conditions (160 lux) compared to very low light intensity conditions (2 lux).

BLYNK Result

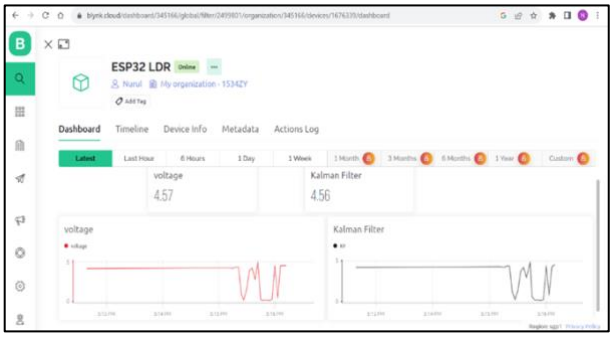

Figure 18. BLYNK for Photodetector data

The presented figure 18. depicts the visual interface of the successful integration of a photodetector sensor with the Blynk platform. Through this platform, users have the capability to monitor and analyze the values generated by the sensor using various available features. The integration process between the photodetector sensor and the Blynk platform involves several stages that contribute to presenting data in a more structured manner. Firstly, the photodetector sensor performs readings that are controlled by an Arduino Mega. The collected data is then transmitted through a serial communication pathway to the ESP32. The ESP32 device acts as an intermediary connecting the sensor data to the Blynk platform.

The Blynk platform is capable of presenting information in a real-time and intuitive manner, enabling users to easily comprehend and interpret the sensor readings. In this interface, photodetector sensor data is presented in the form of graphs, numerical values, or other visual displays, according to user preferences. The integration of the photodetector sensor with the Blynk platform and the utilization of its analysis features represent a significant innovation in data collection and interpretation. The ability to observe data in a structured format, conduct a comprehensive analysis, and gain deeper

insights through this platform can contribute to a better understanding of the observed phenomena.

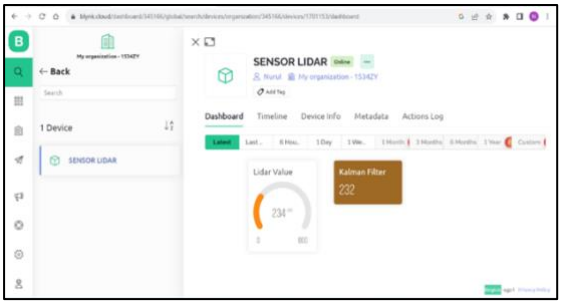

Figure 19. BLYNK for TF-Luna LiDAR data

Displayed portrays the visual interface resulting from the integration of the TF-Luna LiDAR sensor with the Blynk platform. This integration encompasses several technical stages that collectively yield a system enabling efficient monitoring and analysis of sensor data. The process commences with the sensor readings being acquired by the Arduino Mega device. The resultant data is then transmitted through a serial communication pathway to the ESP32 device. The ESP32 serves as a bridge between the sensor and the Blynk platform.

It is crucial to note that the synthesis of hardware elements (such as sensors and microcontrollers) with software aspects (via ESP32 and Blynk) is key to achieving a successful integration. The Blynk platform assumes a central role in visually presenting sensor data, facilitating data visualization in diverse formats as per user preferences. The utilization of the Blynk platform introduces substantial analytical potential. The resulting interface enables real-time monitoring and analysis of data. Users can easily observe changes in sensor values over time, identify trends or patterns, and apply relevant statistical tools to gain deeper insights. This approach aligns with the principles of scientific methodology that emphasize reliable data collection, meticulous analysis, and accurate interpretation.

4. CONCLUSION

In summary, the project has achieved successful real-time integration of sensor data from both the photodetector and TF-Luna LiDAR using the Arduino Mega. The implementation of the Kalman Filter algorithm has proven to be highly effective, providing accurate real-time estimations for the sensors. Among the photodetector variants, the photoresistor outperforms the photodiode in terms of reading accuracy, as indicated by the RMSE values. Remarkably, the KF PR model utilizing 16 LEDs showcases the smallest RMSE value, recorded at an impressive 0.03. Moreover, it has been observed that the TF-Luna LiDAR sensor performs optimally in well-lit conditions, exhibiting superior accuracy compared to low-light conditions. This distinction is evident in the RMSE values, with lux 160 recording an RMSE of 1.41 and lux 2 showing an RMSE of 2.71. Furthermore, the project has successfully demonstrated the visualization of sensor data on the Blynk platform, facilitated by the nodemcu ESP32. These findings collectively underscore the project's accomplishments in enhancing sensor accuracy, real-time data integration, and effective data visualization.

These findings underscore the successful integration of hardware, algorithms, and real-time data processing, leading to enhanced accuracy and effectiveness in sensor estimations. The discerned discrepancies between the two types of Photodetectors and the light-dependent accuracy of the TF-Luna LiDAR sensor offer valuable insights for further refinement and application of similar systems. Furthermore, the data visualization capability on the Blynk platform contributes to comprehensive data monitoring and analysis, enhancing the practicality and utility of the implemented solution.

ACKNOWLEDGMENT

The completion of this research work was made possible through the combined efforts and support of various individuals and organizations, to whom we extend our heartfelt gratitude. We express our deepest appreciation to our supervisor, Dr. Dwi Astharini S.T., M.Sc, for their invaluable guidance, insightful feedback, and constant encouragement throughout the course of this study. The authors gratefully acknowledge the funding provided by the PRG UAI 2023, which was instrumental in supporting and facilitating the research presented in this paper. This financial support enabled the realization of the experimental work, data collection, analysis, and interpretation. We extend our sincere appreciation to PRG UAI

2023 for their contribution to the advancement of knowledge in this field.

REFERENCES

[1] S. U. ,. P. H. J. C. S. Y. D. K. Saeed Ur Rehman, "Visible Light Communication: A System Perspective-Overview and Challenges," *Journal of National Center for Biotechnology*, vol. 19(5), p. 1153, 7 March 2019.

[2] M. Y. Trong-Hop Do, "An in-Depth Survey of Visible Light Communication Based Positioning Systems," *MDPI Journal List*, vol. 16(5), no. https://doi.org/10.3390/s16050678, p. 678, 2016.

[3] C. G. R. B. M. C. W. S. Y. Y. Zhiyu Zhu, "Positioning Using Visible Light Communications: A Perspective Arcs Approach," *journal of arXiv preprint arXiv*, no. https://doi.org/10.48550/arXiv.2204.0811, 2022.

[4] H. L. Y. H. Qu Wang, "Light positioning: A high-accuracy visible light indoor positioning system based on attitude identification and propagation model," *International Journal of Distributed Sensor Networks*, no. https://doi.org/10.1177/1550147718758263, 2015.

[5] F. E. I. G. Yusuf Eroglu, "Adaptive Kalman Tracking for Indoor Visible Light Positioning," *IEEE Military Communications Conference (MILCOM)* , vol. 2019 23(3), no. https://doi.org/10.48550/arXiv.1909.12985, 2019.

[6] F. H. M. G. J. M. M. E. O. Auger, "Industrial applications of the Kalman filter," *I E E E Transactions on Industrial Electronics*, vol. 60(12), no. 10.1109/TIE.2012.2236994, 2013.

[7] "LDR Light Sensor Module LM393 with Digital + Analog Output," 30 July 2023. [Online]. Available: https://probots.co.in/ldr-sensor-module.html.

[8] Atdubotics, "Photodiode sensor module - LM393," [Online]. Available: https://ardubotics.eu/en/sensors/1164-lm393-photodiode-sensor-module.html.

[9] "TF-Luna LiDAR Module - Short-Range Distance Sensor," 01 August 2023. [Online]. Available: https://www.seeedstudio.com/TF-Luna-LiDAR-Module-Short-Range-Distance-Sensor-p-4561.html.

[10] S. W. W. A. H. L. Dwi Astharini, "Improved Extended Kalman Filter For Photodetector Based Visible Light Positioning," *International Journal of Engineering Advanced Research*, vol. Vol. 4(1), pp. 2710-7167, 2022.

[11] M. Fawwaz, "VLC Transmitter and Receiver Point using FPGA Xilinx". Universitas Al-Azhar Indonesia," *Journal of Science*, 2022.